ISBN: 978-3-95450-241-7 ISSN: 2673-5350 doi:10.18429/JACoW-IBIC2022-MOP02

AN OPTICAL DIAGNOSTIC BEAMLINE FOR THE BESSY II BOOSTER

T. Atkinson*, Ji-Gwang Hwang, G. Rehm, M. Ries, G. Schiwietz, S. Wiese
Helmholtz-Zentrum Berlin für Materialien und Energie, Berlin, Germany

Abstract

As part of the global refurbishment of the injector at BESSY II, a new optical beamline has been installed in the booster. This paper covers the conceptual design: incorporating the beamline into an operational facility without downtime, the simulation and expectations of the optical transport line, mechanical installation and commissioning with beam. These first results with the present beam delivery system have already achieved source-point imaging and bunch length measurements using a fast diode. With the additional PETRA cavity installed for this booster upgrade and connection to acquire RF power in the 2022 summer shutdown planned, the bunch length diagnostics are critical. The beamline will also undergo a final mechanical upgrade and then see the installation of a streak camera.

MOTIVATION

In a familiar fashion that characterized 3rd generation light sources across the world, injection into the BESSY II storage ring is from a low energy linac followed by a full energy booster synchrotron.

The present injection scheme is highly reliable [1], but a global upgrade was necessary for the BESSY VSR project [2]. The most prominent aspect with respect to the injector is the evidence that the bunch length on injection into the VSR-storage ring needs to be reduced from its present value, by at least a factor of two in order to keep the high injection efficiencies.

The preferred method to produce shorter bunches from the booster is an upgrade of the existing 500 MHz RF system. An additional 5-cell PETRA cavity driven by a 40 kW transmitter has been installed. In terms of beam commissioning, slowly increasing the total RF gradient is a subtle way to actively control and diagnose the beam in all dimensions.

DESIGN CRITERIA

The design criteria was to keep the optical beamline as short and as simple as possible: use established in-house components and install everything over four shutdowns without any dark-time of the high level source-point diagnostics. In order to minimize the beamline transport length, the output port in the booster was moved in 2020 to a more convenient straight section. This modification to the booster hardware was part of a global reshuffle to accommodate the additional cavities, bunch-by-bunch feedback [3] and redundancy for TopUp current measurement. For beam transport, a total of 7 mirrors each 2 inch in diameter are mounted in the standard HZB holders used throughout the facility, see Fig. 1. Motorized 2-point tilt adjustment is possible.

* terry.atkinson@helmholtz-berlin.de

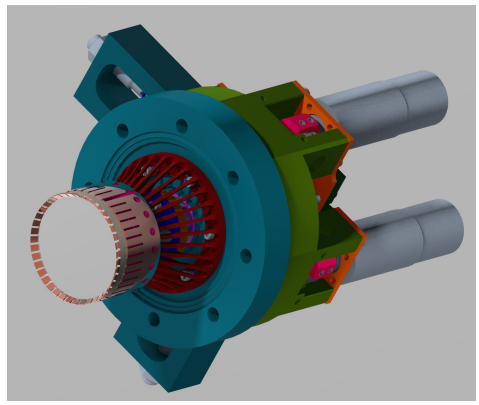

Figure 1: Standard HZB [4] motorized holder for a 2 inch diameter mirror.

The mirrors in the transport line have a surface flatness of lambda/20 to achieve high precision in terms of phase [5]. This allows the source imaging system to measure a spot size close to its diffraction limit.

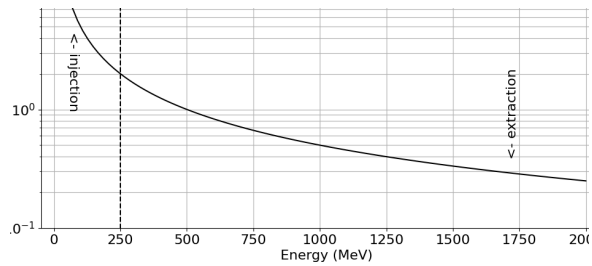

Figure 2: Critical angle of emitted light over the energy ramp of the booster. Without refractive optic, visible light will be outside the angular acceptance for energies < 250 MeV.

From the source, the divergence of the emitted light is corrected using refractive optics, then collimated beam is transported though beamline using the remaining mirrors. There is a 2 degree angle at the output port from the bending magnet.

Noticeably installed is a Intermediate Viewing Point (IVP) consisting of a motorized linear stage and CCD camera at the halfway stage to help align the components. Here both the photon beam and alignment laser were simultaneously observed. Next the beam is transported through the labyrinth out to the optical table. Due to building constraints, a further 20 degree angle is introduced in the labyrinth.

The entire beamline is under vacuum, contains presently one UHV wedged window at the booster output port. This window protects the vacuum in the accelerator and the wedged angle helps to separate spatially unwanted reflection. A second wedged window will be installed next year to com-

Content from this work may be used under the terms of the CC BY 4.0 licence (© 2022). Any distribution of this work must maintain attribution to the author(s), title of the work, publisher, and DOI

ISBN: 978-3-95450-241-7 ISSN: 2673-5350 doi:10.18429/JACoW-IBIC2022-MOP02

Content from this work may be used under the terms of the CC BY 4.0 licence (© 2022). Any distribution of this work must maintain attribution to the author(s), title of the work, publisher, and DOI

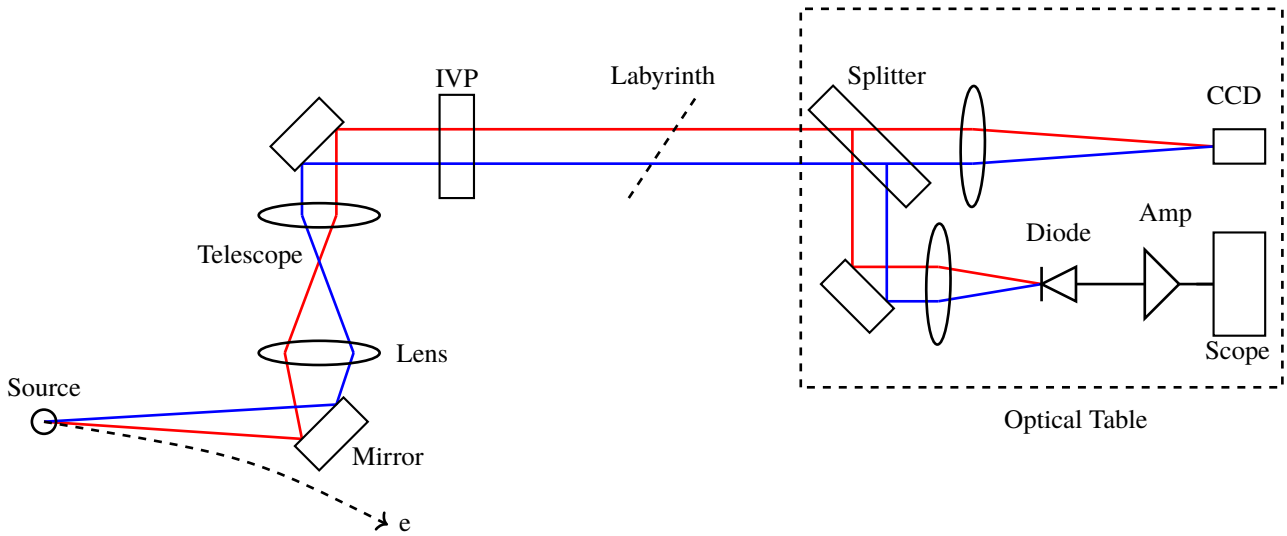

Figure 3: Schematic of the beamline and the present experimental setup on the optical table.

pensate the dispersion effects that may restrict the resolution of beam size diagnostics.

A case study was undertaken to make best use of the fixed distance between the first two mirrors. Here the positions of the lens within the telescope and the resultant chromatic effects for several different lens focus length and type were simulated.

As a guide line, one can estimate that the critical angle: $\theta_c \approx 1/\gamma$ at injection from the 50 MeV linac to be $\theta_c \approx 10$ mrad. With even a larger angular threshold for visible light [6].

Given 10 m from source to final 2 inch (50 mm) diameter mirror, without refractive optics, the light emitted around injection (below 250 MeV, see Fig. 2) will be suppressed below the detection limit. Transmission of the beamline for the same geometric acceptance is improved dramatically when using the telescope.

The design schematic in Fig. 3, highlights the dependence on plain mirrors for beam transport over the 13 m to the optical table. A substantial start-to-end CAD of the whole beamline was developed, see corresponding poster.

By the end of the shutdown in 2021, all fundamental components were installed with the exception of the telescope optic due to delivery problems. The beamline was brought successfully into operation and a single lens was used to generate an image on a CCD camera for the high level diagnostics.

SOURCE-POINT IMAGING

A full characterization of the beamline was not envisaged in this initial set up stage. Emphasis was on stable operation and a beam spot for the high-level diagnostic. Once alignment was achieved, again here the IVP played a vital role, a single 1 m focusing lens some 13 m from the source defined the optic (without telescope and only plane mirrors). The beam diameter at the lens was approximately 20 mm so the half the angular acceptance $\theta_a = 10\,\text{mm} / 13\,\text{m} = 0.77$ mrad. The Abbe limit @600nm $\approx \lambda/(2n \sin\theta_a) = 243\,\mu$m.

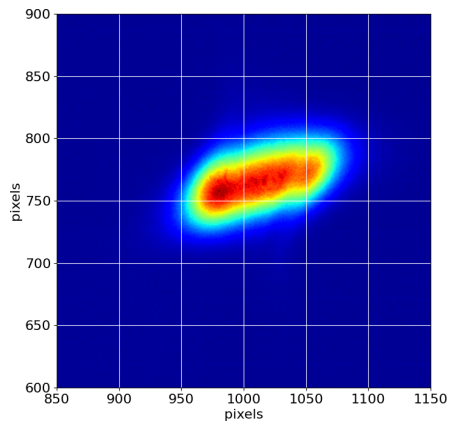

Figure 4: Typical beam image on CCD during machine commissioning whereby alignment optimization and full source-point imaging is ongoing.

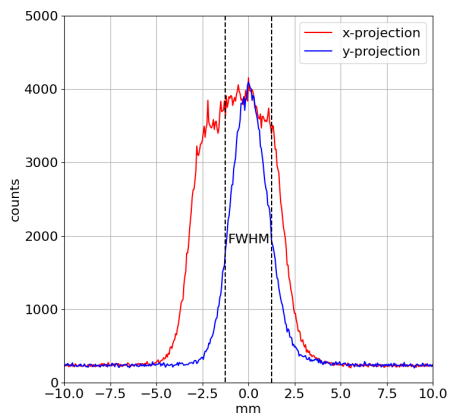

Figure 5: Control system integrated image analysis.

ISBN: 978-3-95450-241-7 ISSN: 2673-5350 doi:10.18429/JACoW-IBIC2022-MOP02

Figure 4 shows a typical beam spot image of the high-level diagnostic (not optimized or at full-focus). The rotation of the profile originated from the angle of the arm in the beamline is compensated by "software". Presently installed is a GT series Allied Vision scientific CCD camera which is designed for imaging in extreme temperatures (from -20 °C up to 65 °C) and fluctuating lighting conditions. In addition, this CDD has good linearity and a pixel size of 4.54 µm. The minimum exposure time is 10 µs, this constitutes to circa 30 turns in the booster.

The Gaussian fit of the vertical projection shown in Fig. 5 suggests $\sigma_y \approx 450\,\mu m$. In this example the beam in the horizontal plane is non-Gaussian and heavily distorted. This was typical during the beamline optimization process and will be addressed again if still apparent after the inclusion of refractive optics and the 2nd wedged window.

The Twiss parameters in the booster at the source can be used to justify some of these early results: Given $\beta_x = 8\,m$, $\beta_y = 3\,m$, $\eta_x = 0.7\,m$ and $\epsilon_{x/y} = 60\,nm$ then $\sigma_x \approx 700\,\mu m$ and $\sigma_y \approx 300\,\mu m$.

BUNCH LENGTH MEASUREMENTS

The installation of a commercial (MSM Metal-Semiconductor-Metal) fast diode from Hamamatsu is a convenient and simple way to measure bunch lengths in the 25 ps regime. Here the diode is powered via a Bias-Tee, the SMA output is connected to a mini-circuit amplifier and the signal is observed on a wideband real-time scope.

Figure 6 shows how the raw data from the scope (black line) is analyzed. In this example, a Gaussian fit of the falling edge of the pulse is taken (red line). This method results in a measured bunch length of 26 ps. Evaluating the rising edge could lead to larger values for the bunch length.

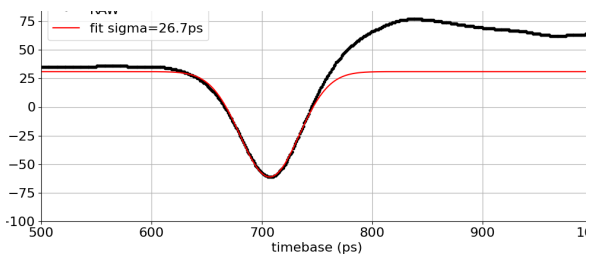

Figure 6: Measurement of pulse on real-time scope. RF cavity voltage cira 604 kV.

The characteristics of the raw data in Fig. 6 are typical for such a system. The overshoot is independent of the amplifier and is a manifestation of the Bias-Tee. The distortions are not caused directly by the inductive resonant circuit $\omega_0 = 1/\sqrt{LC}$ of the Bias-Tee depicted in Fig. 7. The inductance L and capacitance C were measured to be approximately 800 µH and 200 nF respectively which results in a resonant frequency of only 12 kHz. Therefore the very short pulse will not be directly distorted by the operational voltage across the diode via the Bias-Tee. Measurements in the frequency domain such as those described in Ref. [7] to map the insertion loss at high frequencies are still pending. As the light intensity improves through better global alignment and the telescope installation, the amplifier should become redundant and the dedicated studies into this overshoot will continue.

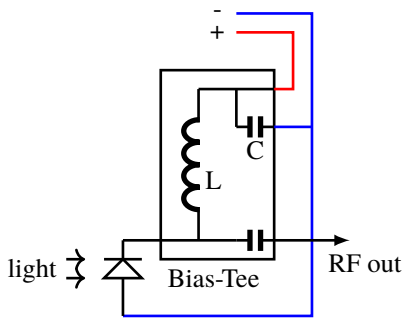

Figure 7: Schematic of fast diode and Bias-Tee [8] circuit diagram.

The specification of the rise-time of the diode is 50 ps. This could be varied using the setup. The rms bunch length at 20 ms in the booster cycle was measured to be $\sigma_t = 26\,ps$ using the scope. Using the Gaussian frequency response notation in Ref. [9] the rise-time is given by:

$$\Delta t_{10-90} = \left(\sqrt{2\ln\frac{1}{0.1}} - \sqrt{2\ln\frac{1}{0.9}}\right)\sigma_t = 1.69\sigma_t = 43\,ps$$

The bandwidth of the diode can be estimated using $BW_{-3dB} * \sigma_t = 0.32$ to be $BW_{diode} = 0.32/\Delta t_{10-90}$.

The bandwidth from the whole system can be approximated using:

$$\frac{1}{\left(BW_{sys}\right)^2} = \frac{1}{\left(BW_{diode}\right)^2} + \frac{1}{\left(BW_{amp}\right)^2} + \frac{1}{\left(BW_{scope}\right)^2} + \ldots$$

where BW_{amp} and BW_{scope} are both 12 GHz. Although the system is bandwidth limited due to the diode, we have the tools to make a Gaussian bandwidth correction to find the 'real' from the 'measured' bunch length on the scope [10].

$$\sigma_{real} = \frac{1}{1.69}\sqrt{(1.69\sigma_t)^2 - \left(\frac{0.32}{BW_{sys}}\right)^2}$$

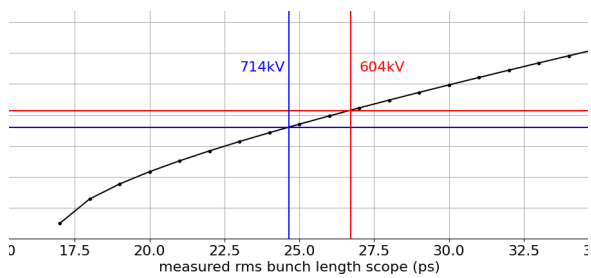

Figure 8: Gaussian bandwidth correction (black line) of measured to real bunch length values at two cavity voltages.

Content from this work may be used under the terms of the CC BY 4.0 licence (© 2022). Any distribution of this work must maintain attribution to the author(s), title of the work, publisher, and DOI

ISBN: 978-3-95450-241-7 ISSN: 2673-5350 doi:10.18429/JACoW-IBIC2022-MOP02

Content from this work may be used under the terms of the CC BY 4.0 licence (© 2022). Any distribution of this work must maintain attribution to the author(s), title of the work, publisher, and DOI

The correction equation is depicted in Fig. 8. Also shown is the experimental data of measured bunch lengths for two different RF voltages in the cavities. In this case the bunch length scales with the voltage given by $\sigma_t \approx 1/\sqrt{V'_{\mathrm{RF}}}$ as expected.

The fast diode is sufficient at this stage in the early operation of the beamline to measure the average bunch lengths at certain points in the booster cycle. The comparison with previous studies [11] is still to be addressed. In this sense, when the cavities are fully commissioned, the further reduction of the bunch length and the non-linear beam dynamics at injection/extraction are better studied using the streak camera, from which the fast diode can be calibrated.

OUTLOOK

The beamline was brought into operation through careful planning without any dark time. Recently the refractive optic was installed and alignment is ongoing. A full characterization of the source-point imaging will be part of a future BSc. project. The adjustments to accommodate for the streak camera will continue in parallel.

REFERENCES

[1] T. Atkinson, P. Goslawski, J. G. Hwang, M. Ries, T. Flisgen, and T. Mertens, "VSR Injector Upgrade at BESSY II", in *Proc. IPAC'18*, Vancouver, Canada, Apr.-May 2018, pp. 4110–4113. doi:10.18429/JACoW-IPAC2018-THPMF030

[2] A. Jankowiak *et al.*, "The BESSY Vsr Project for Short X-Ray Pulse Production", in *Proc. IPAC'16*, Busan, Korea, May 2016, pp. 2833–2836. doi:10.18429/JACoW-IPAC2016-WEPOW009

[3] T. Atkinson *et al.*, "A Longitudinal Kicker Cavity for the BESSY II Booster", in *Proc. IBIC'19*, Malmö, Sweden, Sep. 2019, pp. 150–153. doi:10.18429/JACoW-IBIC2019-MOPP026

[4] FMB Berlin, www.fmb-berlin.de

[5] G. Schiwietz *et al.*, "Bunch-resolved diagnostics for a future electron-storage ring", *Nucl. Instrum. Methods Phys. Res., Sect. A*, vol. 990, p. 164992, 2021. doi:10.1016/j.nima.2020.164992

[6] J. D. Jackson, Chapter 14 in *Classical Electrodynamics*, 1st Edition, Wiley, 1962.

[7] W. J. Song *et al.*, "Development of an On-Line Bunch Length Monitoring System at PLS-II Using an Ultrafast Photodiode", in *Proc. IBIC'21*, Pohang, Korea, Sep. 2021, pp. 384–387. doi:10.18429/JACoW-IBIC2021-WEPP10

[8] ZX85-12G-S+ Mini-Circuits Bias-Tee datasheet, https://www.minicircuits.com/pdfs/ZX85-12G-S+.pdf

[9] S. Bottacchi, *Gigabit Transmission over Multimode Optical Fibre*, pp. 105–106, Wiley, 2006.

[10] J.-G. Hwang *et al.*, "Photodiode Setup for measuring short photon pulses", presented at ARD-ST3 Annual Workshop, 2017, unpublished.

[11] D. Malyutin, T. Atkinson, P. Goslawski, A. Jankowiak, A. N. Matveenko, and M. Ries, "Injection and Bunch Length Studies at the BESSY II Storage Ring", in *Proc. IBIC'17*, Grand Rapids, MI, USA, Aug. 2017, pp. 161–163. doi:10.18429/JACoW-IBIC2017-TUPCC06